Biosynthesis and Characterization of Silver Nanoparticles

Glory Kah
University of Johannesburg
Patrick Njobeh (pnjobeh@uj.ac.za)
University of Johannesburg

Research Article

Keywords: Green nanotechnology, biosynthesis, plants, silver nanoparticles, cost-efficient, Cameroon

Posted Date: March 8th, 2022

DOI: https://doi.org/10.21203/rs.3.rs-1409410/v1

Abstract

In this study, a quick, simple, cost-efficient, and green procedure for silver nanoparticles (AgNPs) biosynthesis was executed at 25°C using 5 easily accessible plants from Cameroon including *Carica papaya, Achillea millefolium, Perilla frutescens*, *Ocimum gratissimum*, and *Garcinia kola.* These plants served as capping and reducing agents, while the $AgNO_3$ salt was the precursor. Initially, bioreduction of metallic Ag^+ to Ag^0 nanoparticles was established via a reduction in pH. Biosynthesis of AgNPs was primarily affirmed visually via a color change of the reaction mixtures with the ultraviolet–visible (UV-Vis) spectroscopy absorption peaks demonstrating that the synthesized particles were indeed AgNPs. X-ray diffractometry (XRD) showed the nanoparticles were crystalline in nature and had negative zeta potential (ζ-potential) values, which indicate they could be naturally stable. The phytochemical and Fourier transform infrared (FTIR) spectroscopic analyses revealed the possible phytochemicals in each aqueous plant extract responsible for reducing the Ag^+ metallic ions to nanoparticles followed by capping and stabilization of the nanoparticles. The high-resolution transmission electrons microscopy (HRTEM) micrographs revealed nanoparticles of varying shapes and sizes. Also, micrographs from the scanning electron microscopy (SEM) showed clouds of polydispersed nanoparticles, which were confirmed by energy dispersive X-ray (EDX) spectroscopy to be highly composed of Ag, with strong optical peaks around 3 kV. The results thus validate that these AgNPs can be efficiently formulated using easily available tropical plants for safe applications in various sectors such as medicine and agriculture.

Introduction

Nanotechnology is perceived as a fast emerging area in modern science and technology, wherein researchers are striving to use cost-effective ways to develop highly efficient materials called nanoparticles [1, 2]. Nanomaterials or nanoparticles refer to materials with nanoscale dimensions and sizes ranging from about 1 to 100 nm [3 - 5]. These materials exhibit novel properties as compared to their bulk counterparts [6, 7] since they have a higher surface-to-volume ratio, which promotes a rapid increase in their reactivity at the molecular level [8].

Naturally, nanoparticles occur as emulsions, pigments, ashes from volcano, and anthropogenic produced like those in exhaust fumes. Nonetheless, the synthesis of nanoparticles has drawn the attention of many scientists because it can help in bridging the gap between large materials and molecular structures of atoms used to produce these materials [9]. Nanoparticles including AgNPs can be synthesized following both “top-down” and “bottom-up” protocols. In the top-down protocol, there is miniaturization of bulk materials into smaller nanoscale structures, whereas the “bottom-up” protocol involves the merging together (building) of atoms/molecules to form nanomaterials. To achieve this, different chemical, physical and biological methods are used [5, 10 - 12]. The physical and chemical methods can generate well-defined and pure nanomaterials. Unfortunately, both these techniques are costly, energy-intensive, require high pressures and temperatures, and could potentially lead to the release of toxic substances to the environment. Besides, the chemical techniques to synthesize nanoparticles make use of large quantities of expensive chemical ingredients such as inorganic solvents, stabilizers, and reducing agents that are asserted to be highly hazardous and toxic [13, 14]. To address these problems, an emerging green nanotechnology approach is suggested [11, 12].

Green nanotechnology focuses on formulating particles and materials at nanoscale dimensions utilizing biological methods and eco-friendly materials while consuming a lesser amount of energy along the process [15]. This green technology is maintained as a novel branch in nanotechnology that amalgamates principles from physicochemical and biological procedures to formulate functionalized nanosized particles [1]. It utilizes microscopic and macroscopic biological sources such as algae, bacteria, fungi, yeasts, seaweeds, and plant extracts from leaves, bark, stem, flower, shoots, seedlings, roots, twigs, peel, fruit, latex, gum, and pods tissue cultures, plants essential oil, and secondary metabolites, as well as biopolymers [10, 14, 16, 17].

Using plants/plants extract to synthesize nanoparticles is more advantageous than microorganisms since the latter requires very special aseptic conditions for pure cell cultures to be maintained. Besides, it is very complex to preserve stabilized cultures when considering growth factors such as temperature, pH, and salinity of cultures [14, 18]. The techniques used to

synthesize nanoparticles using plant/plant extracts are not difficult, extremely cost-effective, and pose no threats to the environment even from their waste. Plant synthesized nanoscale materials are very stable and the speed to synthesis these materials is relatively very fast. Moreover, large quantities of nanoparticles with well-defined nanoparticles of varying shapes and sizes, free of contaminants can be produced [14, 19, 20]. The shapes and sizes of nanoparticles produced via plant-mediated methods can greatly depend on the type of plant used during the process. This is because extracts of plants may contain different combinations and concentrations of reducing organic agents [14]. Moreover, active biochemical compounds from plants such as amino acids, proteins, vitamins, enzymes, alkaloids, phenols, terpenoids, tannins, saponins, and polysaccharides can naturally act as stabilizing and reducing agents, thus helping to accelerate the formulation and stabilization of nanomaterials. This, therefore, implies that no additional costs (stabilizing and reducing agents) are required when using plants to formulate nanoparticles [5, 13, 21].

The biological (green) synthesis of metallic nanoparticles using plants is an encouraging strategy that can help to lessen toxicity associated with different applications as nanoparticles that are formulated via plant-mediated methods are affirmed to be less toxic [19]. Among the noble metallic nanoparticles, AgNPs are nontoxic to human cells when used at low concentrations [22]. Hence, they are widely used in human products such as toothpaste, detergents, soap, cosmetics, shampoos, pharmaceutical, and medical products. Moreover, the biomimetic green synthesis of AgNPs by plants can be suitable for the rapid formulation of AgNPs to successfully meet the excessive current market demand [23]. Therefore, this study[2] explores a rapid, cost-effective, and environmentally safe approach following the greener route to synthesize AgNPs using different tropical plants from Cameroon that seem not to be exploited by researchers in nanoparticle biosynthesis.

[2]This study is part of the author's Master's dissertation in Biotechnology at the University of Johannesburg.

Materials And Methods

Materials

Healthy plant materials that included five tropical plants, *i.e.*, *Carica papaya* (pawpaw), *Achillea millefolium* (Yarrow), *Perilla frutescens* (Perilla), *Ocimum gratissimum* (African basil), and *Garcinia kola* (Bitter kola) (Fig.1) were obtained from Dschang in the West Province of Cameroon in June 2019. The plants were selected based on the fact that they are easily available, inexpensive, and commonly used by the local population as folklore medicine and food. Pure silver nitrate ($AgNO_3$) salt (purity 99.9 %) was sourced from Sigma Aldrich, St. Louis, USA, while distilled water (DH_2O) was obtained from a Milli-Q system (Merck, Johannesburg, South Africa).

Methods

Preparation of Plants and Plant Extracts

The healthy plants were collected and rinsed thrice with pure DH_2O to remove any unwanted particles and dust. Thereafter, the plants were finely cut into smaller pieces and shaded in an oven at 25 °C to dry. The obtained dried plants were sealed tight in labeled plastic bags and transported to South Africa and brought to the Food, and Environment and Health Research Group (FEHRG) laboratory, at the University of Johannesburg. The dried plant samples were ground to powder using a mechanical blender (IKA WERKE M20 Batch Mill, Merck, Staufen, Germany) then stored in well-labeled airtight clean bottles.

To obtain the plant extracts water, known to be highly polar for simple extraction of highly polar phytochemicals from plants [14] was used as the extraction solvent. Accordingly, 10 g of each powdered plant sample were transferred into a 250 mL labeled beaker containing 100 mL of DH_2O and allowed on a benchtop shaker for 24 hours before boiling for 15 minutes using a heating plate under magnetic stirring (Heidolph MR 3001 K, Magnetic Stirring Hotplate, Merck, Schwabach, Germany). The plant extracts were filtered twice using filter paper (Whatman No. 1) to get rid of particulates.

Phytochemical Analysis

The phytoconstituents of the 5 plants used in the biosynthesis of AgNPs were determined using standard procedures as demonstrated by Yadav and Agarwala [24], Samejo et al. [25], Yadav et al. [26], and Baoduy et al. [27].

Flavonoids (Alkaline Reagent Test)

Two mL of 2 % sodium hydroxide (NaOH) were mixed with 2 mL of each crude aqueous extract in a 15 mL glass test tube. Yellow precipitates developed which changed to colorless as drops of diluted hydrochloric acid (HCl) were added, indicating the presence of flavonoids [24].

Carbohydrates (Iodine Test)

Aqueous crude plant extracts of volume 2 mL were mixed with 2mL of iodine solution. The production of a dark blue coloration denoted the presence of carbohydrates [24].

Test for Glycosides (Keller-Kiliani Test)

One mL of acetic acid (CH_3COOH), 4 drops of concentrated sulphuric acid (H_2SO_4), and 4 drops of ferric chloride ($FeCl_3$) were added into 2 mL of each crude extract in a 15 mL glass test tube. The formation of greenish-blue coloration denoted the presence of glycosides [25].

Saponins (Frothing Test)

One gram of each powdered plant sample were boiled in 10 mL of DH_2O in a 50 mL Erlenmeyer conical flask and filtered. The presence of saponins was established based on the formation of persistent froths [25].

Tannins (Braymer's Test)

In a 15 mL glass test tube, 2 mL of each extract were added to 2 mL of DH_2O, followed by 3 drops of $FeCl_3$ (5%). The formation of a green coloration confirmed the presence of tannins [26].

Anthocyanins

In a 15 mL glass test tube, 2 mL of each extract were mixed to 2 mL of HCl (2N) and ammonia (NH_3).The formation of a pinkish-red coloration which turned blue-violet revealed the presence of anthocyanin [26].

Coumarins

Two mL of each extract were added to 2 mL NaOH (10%) in a 15 mL glass test tube. Coumarin was affirmed based on the appearance of a yellow coloration [26].

Anthraquinones (Borntrager's Test)

In a 15 mL glass test tube containing 5 mL NH_3 (10%) and 3 mL benzene (C_6H_6) 3 mL of each extract were added and mixed. Anthraquinone was affirmed following the appearance of a pinkish to red coloration at the layer containing NH_3 [26].

Terpenoids (Salkowski Test)

In different tests tubes with 5 mL of each plant extract, 2 mL of chloroform ($CHCl_3$) were added followed by 3 mL of concentrated H_2SO_4. The formation of a reddish-brown coloration at the interface with $CHCl_3$ denoted the presence of terpenoids [27]

Phenols (Ferric Chloride Test)

One mL of each extract were treated with 4 drops of $FeCl_3$ (1%) in a 15 mL round bottom glass test tube. The presence of phenols was established based on the production of blue to black coloration [27].

Steroids (Lieberman-Burchard's Test)

Two mL of aqueous plant extracts were added to 2 mL ($CHCl_3$). To this mixture, 5 drops of concentrated H_2SO_4 and 10 drops of CH□COOH were added and gently mixed in a 15 mL glass test tube. The formation of a red color which gradually changed to blue, then to green denoted the presence of steroids [27].

Biosynthesis of Silver Nanoparticles

Pure $AgNO_3$ salt was used to prepare a 5 mM aqueous solution of $AgNO_3$ at room temperature. Thereafter, 10 mL of each plant extract were added into a 250 mL Erlenmeyer conical flask containing 90 mL 5 mM aqueous solution of $AgNO_3$maintained at 25 °C in an incubator for 24 hours until complete synthesis of AgNPs and purified by centrifugation. The solutions were poured into 50 mL centrifuge tubes and centrifuged at 12000 rpm and 25 °C for 20 minutes, supernatants discarded, and sediments washed twice in DH_2O. The sediments containing purified AgNPs were frozen at -70 °C for 24 hours and frozen samples lyophilized for 48 hours using a benchtop freeze-dryer (Telstar Lyoquest Freeze Dryer, Tokyo, Japan).

Characterization of Silver Nanoparticles

The formulated AgNPs were characterized using analytical techniques that included pH analysis, color change, ultraviolet–visible (UV-Vis) spectroscopy, Fourier transform infrared (FTIR) spectroscopy, scanning electron microscopy (SEM), energy dispersive X-rays(EDX) spectroscopy, high-resolution transmission electron microscopy (HRTEM), X-ray diffractometry (XRD), and zeta potential (ζ-potential). A benchtop pH meter (OHAUS, Starter 3100M, New Jersey, USA) was used to measure the pH of the aqueous plant extracts and that of 5 mM $AgNO_3$ solutions before the synthesis of AgNPs. After, the changes in pH in each reaction mixture during the formulation of AgNPs were also measured [28].

UV-Vis spectroscopy analysis of AgNPs was done 24 hours after mixing the plant extracts with 5 mM aqueous $AgNO_3$ solution. That of the aqueous plant extracts was also performed as controls. One mL of AgNPs solution (suspension) was obtained after 24 hours and then mixed with 3 mL of DH_2O. Then, 2 mL of the prepared solution was poured into a UV grade silica cuvette and scanned at a resolution of 1 nm using a UV-Vis spectrophotometer (UV-2450, Shimadzu, Tokyo, Japan) set at wavelengths ranging from 300 to 800 nm.

Fourier transform infrared (FTIR) spectroscopy technique was exploited to determine the functional groups that may be responsible for the bioformulation of AgNPs. Lyophilised samples consisting of plant extracts (control) and the biosynthesized AgNPs were used. As done, each of the lyophilized samples was ground with potassium bromide (KBr) of FTIR grade (Sigma Aldrich, St. Louis, USA) (1:100, w/w) using a pellet press (Manual Hydraulic press, Specac Ltd, Orpington, UK) and then analyzed using FTIR spectroscopy instrument (PerkinElmer, Spectrum 100 FTIR spectrometer, Shelton , USA). The spectrum was read within the range of 4000 to 400 cm^{-1} in a transmittance mode running at a 4 cm^{-1} resolution [23, 29].

Scanning electron microscopy (SEM) and energy dispersive X-ray (EDX) spectroscopy analyses of AgNPs were performed using thin films of AgNPs. Powered films of AgNPs samples were evenly distributed to cement on carbon tapes attached to SEM aluminum sample holders and coated with carbon for 45 minutes in a benchtop SEM sputter carbon cord coater (Quorum Q300T ES, East Sussex, UK). The coated samples were analyzed using a TESCAN (SEM, TESCAN Vega 3, Brno, Czech Republic) set with 15 mm working distance, and 20 kV accelerating voltage, and connected to a secondary electron (SE) detector. For EDX spectroscopy, the same samples used for SEM analysis were then analyzed at 20 kV using the micro X-ray analyzer (X-MAX EDX Oxford instruments, Oxford, UK) connected to the SEM TESCAN system.

High-resolution transmission electron microscopy (HRTEM) was used to determine the shapes and sizes of the synthesized AgNPs. Half a gram of biosynthesized AgNPs powdered samples was each poured into 10 mL of sterile DH_2O in a 15 mL

conical tube, then sonicated for 20 minutes using an ultrasonic bath (Siel UST 2, 8-100, 120 W, Siel Ltd., Gabrovo, Bulgaria) to avoid aggregation of particles. After sonication, 5 µL of each of the aqueous samples containing the nanoparticles was dropped on the dark sides of a fine 200 mesh copper grids coated with carbon. The grids were air-dried overnight at room temperature before loading on the HRTEM sample holder. The HRTEM machine (JEOL JEM-2100, 80-200 kV, JEOL Ltd. Tokyo Japan) was then used to capture micrographs of the AgNPs at magnifications of 50 and 100 nm [17].

Also, X-ray diffractometry (XRD) analysis of the synthesized AgNPs was done, wherein homogenized finely ground samples were mounted on the XRD quartz plates and positioned on the XRD sample holder and analyzed using an X-ray instrument (Philips X'Pert Pro x-ray diffractometer, Almelo, The Netherlands) connected to an X'celerator detector. The instrument operated with scans done at an angle of 2θ and an angular range of 4° to 90° using a Cu Kα radiation of 1.5443 ˚A. The generator was set with a current of 30 mA and voltage of 40 Kv [30].

For the zeta potential (ζ-potential) analysis, AgNPs powdered samples were diluted with 0.3 mM phosphate buffer saline (PBS) of pH 7.40 to give 75 µg/mL of AgNPs. The AgNPs solutions were then sonicated for 20 minutes. Each sonicated sample was poured into the zeta dip cell and analyzed using Malvern Zetasizer 2000 (Malvern, Worcestershire, UK) supplied with a stable source of laser beam [31].

Results And Discussion

Phytochemical Analysis

The phytochemical constituents of the plant extracts studied are summarized in Table 1. The concentration of phytochemicals in the tested plant extracts were qualitatively determined based on the color intensity observed in the reaction mixture as stipulated by the analytical procedure [24 - 27]. We noted that phenols, saponins, steroids, tannins, anthocyanins, coumarins, terpenoids, and flavonoids were present in all tested extracts of *Ocimum gratissimum*. In *Achillea millefolium* extract; phenols, saponins, anthraquinones, coumarins, flavonoids, and terpenoids were recovered. In *Perilla frutescens;* phenols, saponins, steroids, anthocyanins, and terpenoids were found. *Carica papaya* extract had phenols, saponins, steroids, coumarins, flavonoids, and terpenoids. While Phenols, saponins, steroids, coumarins, flavonoids, terpenoids, and carbohydrates were identified in *Garcinia kola.* Besides, flavonoids were found at moderate concentrations in *Ocimum gratissimum* extract, whereas coumarins were recovered at moderate concentration in *Achillea millefolium* and *Carica papaya* extracts than in other plant extracts. Also, steroids were found in moderate concentrations only in *Garcinia kola* (nuts) and tannins were at the highest concentrations in these nuts than any of the analyzed plants. Carbohydrates were only recovered in *Garcinia kola*. Even though glycosides were not found in any of the plant extracts, terpenoids, flavonoids, and phenols were instead present in all plant extracts tested. These phytochemical analytical results indicate that each plant contains a blend of different phytochemicals. These phytochemicals could be of important medical value and are asserted to play a major role in reducing and stabilizing Ag ions during the bioformulation of AgNPs [11]. Also, terpenoids, phenols, and flavonoids, which were affirmed present in all analyzed plant extracts, can be responsible for stabilizing and capping AgNPs [23]. Besides, the transformation of flavonoids to keto-enol tautomer might occur leading to the release of free active molecules of hydrogen, which might accelerate the reduction of Ag^{+} to Ag^{0} nanoparticles [32]. Moreover, some of the identified phytochemicals such as phenols and terpenoids have polar groups including OH and CO, which can bind to the surface of Ag ions. These groups (OH and CO) may also play a vital role in the mechanisms involved in the bioreduction of metallic Ag [33].

Table 1 Phytochemical results of the plants used in the biosynthesis of AgNPs

		Plant				
S. No.	**Phytochemical**	*Ocimum gratissimum* (African basil)	*Achillea millefolium* (Yarrow)	*Perilla fructescens* (Perilla)	*Carica papaya (Pawpaw)*	*Garcinia kola* (Bitter kola)
1	Phenols	+	+	+	+	+
2	Saponins	+	+	+	+	+
3	Steroids	+	-	+	+	++
4	Tannins	+	+	+	+	+++
5	Glycosides	-	-	-	-	-
6	Anthocyanins	+	-	+	-	-
7	Anthraquinones	-	+	-	-	-
8	Coumarins	+	++	-	++	+
9	Terpenoids	+	+	+	+	+
10	Flavonoids	++	+	+	+	+
11	Carbohydrates	-	-	-	-	+

(**Notation: -** = Absent of phytochemical, **+** = Presence of phytochemical, **++** = Moderate concentration of phytochemical, **+++** = high concentration of phytochemical).

Color Change

Also, color change in the reaction mixture was observed. The first visible clue that nanoparticles are formed in a reaction mixture is a color change [34]. Changes of color in the reaction mixtures were perceived macroscopically within 1 to 60 minutes in all the reaction mixtures. The color intensity in each reaction mixture gradually changed from a colorless solution of $AgNO_3$ to varying colors over time (Table 3 and Fig. 2).

Table 3 Color observed in the reaction mixture during biosynthesis of AgNPs

Solution	Before reduction	1 to 60 minutes after	24 hours after
Aqueous 5 mM solution of $AgNO_3$	Colorless	-	-
Achillea millefolium leaf extract	Brown	-	-
Perilla frutescens leaf extract	Dark green	-	-
Garcinia kola extract	Yarrow	-	-
Carica papaya leaf extract	Dark green	-	-
Ocimum gratissimum leaf extract	Dark green	-	-
Achillea millefolium leaf extract + 5 mM $AgNO_3$	-	Brown	Dark brown
Perilla fructescens leaf extract + 5 mM $AgNO_3$	-	Brown	Dark
Garcinia kola extract + 5 mM $AgNO_3$	-	Pale yarrow	Brown
Carica papaya leaf extract + 5 mM $AgNO_3$	-	Yellow brown	Dark
Ocimum gratissimum leaf extract + 5 mM $AgNO_3$	-	Brown	Dark brown

However, beyond 24 hours, no considerable color change was perceived in the reaction mixture (Fig 2). This insinuated that the reduction of Ag^+ to Ag^0 was complete. The final color observed in the presence of each plant extract after 24 hours was brown for *Garcinia kola*, dark brown for *Achillea millefolium* and *Ocimum gratissimum,* and dark for *Achillea millefolium* and *Carica papaya*.). The change in color in the reaction mixture during the synthesis of AgNPs using plant extracts is attributed to the fact that biologically active compounds found in plant extracts at different concentrations can reduce Ag^+ metallic ions to Ag^0. This is a clear evidence that AgNPs are formulated [28]. Besides, the induced stimulation of superficial plasmon vibrations of AgNPs can also be responsible for the development of color during the synthesis of AgNPs [35].

pH Variation

A general reduction in pH was noted in the mixture after 10 mL of each plant extract was added to 90 mL of 5 mM aqueous solution of $AgNO_3$ (Table 2). The reduction in pH ranged from 0.10 to 0.97 with the greatest reduction recorded in the reaction mixture with *Carica papaya* leaf extract were noted. The decreases in pH indicate a reduction of $AgNO_3$ to Ag^0 nanoparticles in the presence of each plant extract. Also, decreases in pH in the reaction mixture have been reported during the formulation of AgNPs using leaf extracts of *Syzygium cumini* and *Tecomella undulate.* In the reaction mixture with *Syzygium cumini* extract, pH slightly dropped from 4.84 to 4.72 [36] whereas, with *Tecomella undulate* extract, pH decreased from 6.5 to 5.5 [28]. The variations in pH could also play an essential role in the formulation of nanoparticles with different sizes and shapes. For instance, Mishra et al. [37] substantiated that the synthesis of AgNPs using leaf extract of *Averrhoa carambola* led to the formation of spherical nanoparticles at pH range from 2.00 to 7.00. Whereas at higher pH of 8.00, nanoparticles with other shapes, which include hexagons, spheres, triangles, squares, and rectangles were synthesized [37]. These documented results correlate with those obtained in this study as the HRTEM analysis further confirmed the synthesized AgNPs had varying shapes and sizes.

Table 2 pH variation recorded during biosynthesis of AgNPs

pH of Solution	pH before Solution	pH after reduction	reduction
Aqueous 5 mM solution of $AgNO_3$	6.00	-	-
Carica papaya leaf extract	7.83	-	-
Achillea millefolium leaf extract	6.06	-	-
Perilla frutescens leaf extract	8.12	-	-
Ocimum gratissimum leaf extract	7.30	-	-
Garcinia kola extract	6.00	-	-
Carica papaya leaf extract + 5 mM $AgNO_3$	-	6.00	5.03
Achillea millefolium leaf extract + 5 mM $AgNO_3$	-	5.10	5.00
Perilla frutescens leaf extract + 5 mM $AgNO_3$	-	7.00	6.21
Ocimum gratissimum leaf extract + 5 mM $AgNO_3$	-	5.40	5.16
Garcinia kola extract + 5 mM $AgNO_3$	-	5.00	4.82

UV-Vis Spectroscopy

The UV-Vis spectra obtained using colloidal solutions of biosynthesized AgNPs and the plant extracts (controls) are shown in Fig. 3 with single absorption peaks centered at 441, 429, 451, 438, and 447 nm. These peaks correspond to *Achillea millefolium, Perilla frutescens, Garcina kola, Carica papaya,* and *Ocimum gratssimum* AgNPs. These spectrum absorption peaks for the biosynthesized AgNPs correspond to the surface plasmon resonance (SPR) formed as oscillating electrons from AgNPs come in resonance with light waves [38, 39]. This is an indication that addition of each plant extract to $AgNO_3$ aqueous solution stimulated a transition of electrons, resulting in Ag^{2+} ions being reduced to Ag^0 [38,40]. Moreover, the broadening nature of peaks for all the formulated AgNPs, as can be seen in the UV-Vis spectra indicates that the nanoparticles are polydisperse and this greatly correlates with the HRTEM results.

FTIR Spectroscopy

The FTIR spectra of *Achillea millefolium*, *Perilla frutescens, Ocimum gratissimum*, *Carica papaya,* and *Garcinia kola,* alongside their biosynthesized AgNPs are shown in Fig. 4. The spectra of *Achillea millefolium* extract and *Achillea millefolium* AgNPs (Fig. 4A) showed peaks at 3400.04 and 3130.79 cm^{-1} (O—H stretch from alcohol or phenol), 2930.02 cm^{-1} (C—H stretch of alkanes), 1611.71 and 1596.05 cm^{-1} (N-H stretch of amine), 1400.86 and 1399.17 cm^{-1} (C-H stretch of alkanes), 1077.10 and 1079.74 cm^{-1} (C-OH stretch), 617.39, 539.38 and 531.55 cm^{-1} (C-Cl stretch of alkyl halides).

The IR spectra of *Perilla frutescens* extract and AgNPs from *Perilla frutescens* (Fig. 4B) have peaks at 3400.72 and 31778.67 cm^{-1} (O—H stretch from alcohols or phenols), 2345.39 cm^{-1} (–C=C- stretch of alkynes), 1603.76 cm^{-1} (N-H stretch of amines), 1400.64 cm^{-1} (C-H stretch of alkanes), 1055.00 cm^{-1} (C-OH stretch) and 617.39 cm^{-1} (C-Cl stretch of alkyl halides). For *Ocimum gratissimum* extract and AgNPs synthesized using *Ocimum gratissimum* (Fig. 4C), the IR spectra have peaks at 3399.90, 3210.95, and 3129.70 cm^{-1} (O—H stretch from alcohols or phenols), 2930.02 cm^{-1} (C—H stretch of alkanes), 2345.69 cm^{-1} (–C=C- stretch of alkynes) 1610.36 and 1595.75 cm^{-1} (N-H stretch of amines), 1399.17 cm^{-1} (C-H stretch of alkanes), 1118.57, 1067.51 and 1032.16 cm^{-1} (C-OH stretch) 705.94, 618.35, 617.48, and 533.93 cm-1 (C-Cl stretch of alkyl halides).

In the case of *Carica papaya* extract and *Carica papaya* AgNPs and (Fig. 4D), IR spectra peaks appeared at 3357.42 and 3138.07 cm^{-1} (O—H of alcohols or phenols), 2939.04. 2932.46 and 2848.17 cm^{-1} (C—H stretch of alkanes), 2346.26 and 2342.87 cm^{-1} (–C=C- stretch of alkynes) 1647.54 and 1638.38 cm^{-1} (N-H stretch of amine), 1400.64 and 1396.92 cm^{-1} (C-H bend), 1257.59 cm^{-1} (C-N stretch of amines), 1058.55 and 1036.33 cm^{-1} (C-OH stretch), 917.74, 816.92 and 779.05 cm^{-1} (C-H bend), 670.12, 615.48 and 540.11 cm^{-1} (C-Cl stretch of alkyl halides).

The IR peaks for *Garcinia kola* extract and *Garcinia kola* AgNPs were seen at 3391.14 and 3136.50 cm^{-1} (O—H of alcohols or phenol), 2937.14 and 2922.28 cm^{-1} (C—H stretch of alkanes) 1634.22 cm^{-1} (N-H stretch of amide), 1401.17 cm^{-1} (C-H bend), 1260.08 cm^{-1} (C-N stretch amines), 1056.12 and 1024.04 cm^{-1} (C-OH stretch), 901.45, 831.01 and 705.08 cm^{-1} (C-H bend), 627.55, 562.84 and 527.10 cm^{-1} (C-Cl stretch of alkyl halides) (Fig. 4E).

The absorption peaks (Fig. 4A, B, C, D, and E) suggest that phytochemicals with functional groups such as OH (alcohol and phenol), C-H (alkanes), –C=C- (alkynes), =C-H (alkenes), N-H (amines), C-OH (carbonyls) and C-Cl (alkyl halides) were present in all the plant extracts and could be involved in the biosynthesis of AgNPs. These results are similar to previously reported in the literature that revealed phenols, alcohols, alkanes, alkynes, carbonyls, protein, and other metabolites inform extracts of some plants can interact with metallic ions during the formation of nanoparticles [33, 41, 42]. In addition, the results insinuate that the biosynthesized AgNPs could be enclosed by metabolites and proteins coming from the plants. For example, the identified IR peaks corresponding to the carbonyl (C-OH) group present in all samples analyzed, could be radiating from proteins and residual amino acids and are alluded to strongly bind to metal ions. Moreover, proteins can function as capping agents for AgNPs and hence, stabilize the emulsion and also prevent agglomeration, implying that bioactive functional molecules from the plant extracts have a dual function in the synthesis and stabilization of AgNPs [41].

When comparing the absorbance peaks of these plant extracts (control) to their biosynthesized AgNPs (Fig. 4A, B, C, D, and E), some shifts in peaks can be seen. This is probably due to the re-arrangement of functional groups found in the plant extracts as the synthesis of AgNPs takes place. For instance, the general shift (shift to a lower wavelength) in peaks of the hydroxyl group was noted and can be considered there was oxidation of this group during the formation of AgNPs with increased production of a carbonyl group [43]. Likewise, when comparing the IR peaks for the 5 biosynthesized AgNPs (Fig. 4.3F), intense absorbance peaks were seen around 3137.21 cm−1 (O—H of alcohol or phenol), 1634.22 cm−1 (N-H stretch), 1400.64 cm−1 (C-H bend), and 1055.00 cm−1 (C-OH stretching). The functional groups associated with these peaks suggest that major phytochemicals such as flavonoids, terpenoids, and phenols could be considerably involved in the formulation of AgNPs [44]. Equally, phytochemical analysis confirmed the presence of flavonoids, terpenoids, and phenols in all plant extracts.

SEM and EDX Analysis

The SEM micrographs (Fig. 5a, c, e, g, and i) show clouds of well-capped and homogenous nanoparticles of different sizes and shapes. The larger nanoparticles seen in the micrographs can be due to the aggregation of smaller particles, which could be linked to the SEM analytical procedure used [45]. However, the HRTEM results of this study were then used to confirm the shapes and sizes of the synthesized nanoparticles. Besides, the EDX results (Fig. 5b, d, f, h, and j) further established that the clouds of nanoparticles seen in the SEM micrographs are AgNPs. This is because EDX data for similar samples had very strong optical absorption peaks at 3 keV, which corresponded to the surface plasmon resonance of metallic Ag. The strong peaks affirmed the formation and purity of the AgNPs. However, other weak optical peaks for C, O, Cl, Cu, and P were observed. These weak peaks may have originated from organic biomolecules in these plant extracts used during the biosynthesis of AgNPs [45].

HRTEM Analysis

The HRTEM micrographs obtained at 50 and 100 nm magnifications showed polydispersed nanoparticles with different shapes and sizes (Fig. 6a, a1, b, b1, c, c1, d, d1, e, and e1). This could be linked to the nature and quantity of the capping

agents found in each plant extract. The micrographs of AgNPs formulated using *Garcinia kola* showed spherical, triangular, and hexagonal shaped AgNPs (Fig. 6a and a1). The size distribution histogram (Fig. 6a2) confirmed that the sizes of the nanoparticles ranged from 5 to 45 nm (mean size of 19.1 nm). The nanoparticles with the highest frequency were between 10 to 15 nm in sizes similar to those documented by Abdi et al. [13]. The micrographs (Fig. 6b and b1) for *Carica papaya* AgNPs revealed that the nanoparticles were tetragonal, hexagonal, and spherical with histogram (Fig. 6b2) indicating the sizes of the nanoparticles were in the range of 20 to 120 nm with a mean size of 67.5 nm. The particles of sizes 60 to 70 nm had the highest frequency. In the case of *Achillea millefolium* AgNPs*,* the micrographs (Fig. 6c and c1) showed spherical shaped AgNPs. The histogram (Fig. 6c2) disclosed that the average size of nanoparticles was 10.9 nm (range: 4 to 18 nm) with the most frequent ranging from 9 to 10 nm. Furthermore, the HRTEM micrographs of AgNPs synthesized from *Perilla frutescens* taken at 50 and 100 nm magnifications (Fig. 6d and d1) revealed the presence of tetrahedral, triangular, oblong, and spherical AgNPs. The histogram (Fig. 6d2) indicated that the nanoparticles were ranging from 0 to 50 nm in sizes and with an average size of 26.1 nm. The most frequent nanoparticles were those with sizes ranging from 20 to 25 nm. For *Ocimum gratissimum* AgNPs (Fig. 6e and e1), the micrographs showed spherical and oblong nanoparticles. The histogram (Fig. 6e2) confirmed that the nanoparticles were ranging from 6 to 33 nm in sizes with a mean size of 15.8 nm and the most frequent particles were ranging from 12 to 14 nm in sizes.

XRD diffractometry

The crystalline nature of AgNPs was determined by XRD analysis. The obtained XRD patterns for the analyzed samples recorded at 2θ are shown in Fig. 7. The XRD pattern of *Achillea millefolium* AgNPs showed intense peaks at 38.1°, 44.3°, 64.4°, 77.3°, and 81.5°, that correspond to (111), (200), (220), (311), and (222) lattice planes, respectively (Fig. 7a). This XRD data for *Achillea millefolium* AgNPs match with standard data from the International Centre for Diffraction Data (ICDD) for Ag with code No. 03-065-2871. The XRD pattern for *Perilla frutescens* AgNPs (Fig. 7b) had major XRD peaks at 38.0°, 44.2°, 64.4°, 77.3°, and 81.4° that correspond with lattice planes at (111), (200), (220), (311), and (222), respectively. This data equally match with the ICDD for Ag with reference code No. 04-001-2617. Fig. 7c is the XRD pattern for *Ocimum. gratissimum* AgNPs with intense peaks at 38.1°, 44.3°, 64.4°, 77.4°, and 81.5° that corresponds with Ag lattice planes at respectively, (111), (200), (220), (311), and (222). This XRD data matches with standard data of the ICDD for Ag with reference code No. 04-004-6437. The XRD pattern for *Carica papaya* AgNPs (Fig. 7d) had intense peaks at 38.0°, 44.2°, 64.3°, 77.3°, and 81.4° corresponding with lattice planes of Ag at (111), (200), (220), (311), and (222), respectively. This data agrees with the ICDD for Ag with reference code No. 04-014-0266. For *Garcinia kola* AgNPs, XRD peaks were observed at 37.9°, 44.1°, 64.2°, 77.0°, and 81.2° (Fig 7e). These peaks correspond to (111), (200), (220), (311), and (222) lattice planes of Ag. The obtained data correlate well with ICDD for Ag (reference code No: 04-003-7118). These XRD patterns all had intense peaks at around 38.0°, 44.0°, 64.0°, 77.0°, and 81.0°, which are assigned with lattice planes of Ag at 111, 200, 220, 311, and 222, respectively (Fig. 7a, b, c, d, and e). These peaks can be indexed as crystalline AgNPs with face-centered cubic (FCC) lattice. The intense diffraction peaks (Bragg reflections) indicate that the x-ray scattering spots are radiating from crystalline materials found in the analyzed samples. These crystalline materials are inorganic compounds, which certainly are Ag nanomaterials [46]. Nonetheless, some of the samples had unassigned peaks, which were denoted (⁎) (Fig. 7a, b, and c). These unassigned peaks (⁎) could be coming from other crystalline metalloproteins/bioorganic composites present in the plant extracts used for the biosynthesis of AgNPs [47, 12].

ζ-potential Analysis

The ζ-potential values for all the formulated AgNPs were negative (-13.4, -14.3, -23.0, -16.3 and -22.4) for *Garcinia kola, Carica papaya, Achillea millefolium, Perilla frutescens,* and *Ocimum gratissimum* AgNPs, respectively (Fig. 8a, b, c, d, and e). The findings are in agreement with other studies wherein negative values for ζ-potential obtained for AgNPs were biosynthesized using plant extracts [48, 49]. These negative zeta values suggest that the biosynthesized AgNPs are superficially negatively charged and stable demonstrating satisfactory evidence that the AgNPs could have strong surface charges that can hinder agglomeration. Hence, these negatively charged nanoparticles could always be apart from each other in solution due to

Coulomb explosion. Moreover, the obtained negative values for ζ-potential affirmed the effectiveness of the bioactive capping agent from plant extracts to stabilize the formulated AgNPs [50, 51].

Conclusions

The use of green nanotechnology in the biosynthesis of metallic nanoparticles such as AgNPs using plant extracts has numerous advantages since it is rapid, simple, cost-effective, and eco-friendly. In this study, the biosynthesis of AgNPs was effectively achieved from bioreduction of aqueous $AgNO_3$ using *Carica papaya, Achillea millefolium, Perilla frutescens*, *Ocimum gratissimum*, and *Garcinia kola* from Cameroon. The different techniques used for characterization confirmed the formation of stable AgNPs with varying shapes and sizes. AgNPs with the smallest mean size of 10.9 nm were generated using *Achillea millefolium.* This was made possible owing to the bioactive compounds present in these plants. The wide application of such biosynthesized AgNPs in the medical and agriculture sectors is necessary considering as these nanoparticles are particularly eco-safe and economically viable.

Abbreviations

AgNPs
Silver nanoparticles
UV-Vis
Ultraviolet-visible spectroscopy
FTIR
Fourier transform infrared spectroscopy
SEM
Scanning electron microscopy
EDX
Energy dispersive X-rays spectroscopy
HRTEM
High-resolution transmission electron microscopy
XRD
X-ray diffractometry
ζ-potential
zeta potential
distilled water
DH_2O
ICDD
International Centre for Diffraction Data

Declarations

Acknowledgments

This study was financially supported by the National Research Foundation (NRF) of South Africa; the University Research Committee (URC) of the University of Johannesburg, South Africa.

Author Details

[1]Department of Biotechnology and Food Technology, Faculty of Science, University of Johannesburg, P.O. Box 17011, Doornfontein Campus, Gauteng, South Africa.

Authors' Contributions

GK designed the study, prepared and characterized the nanoparticles, analyzed the data, and drafted the manuscript. PN sourced for funding, supervised the project, revised and corrected the manuscript. The final manuscript was read and approved by all the authors.

Availability of Data and Materials

The datasets supporting the findings of this study are available from the corresponding authors upon reasonable request.

Competing Interests

The authors declare that they have no competing interests.

Ethics Approval and Consent to Participate

Not applicable.

Consent for Publication

The authors agree that the manuscript should be published.

References

1. Keat CL, Aziz A, Eid AM, Elmarzugi NA (2015) Biosynthesis of nanoparticles and silver nanoparticle. Bioresourc Bioprocess 2(47):1–11
2. Thakkar KN, Mhatre SS, Parikh RY (2010) Biological synthesis of metallic nanoparticles. Nanomedicine 6(2):257–262
3. Gebreslassie YT, Gebretnsae HG (2021) Green and cost-effective synthesis of Tin Oxide nanoparticles: a review on the synthesis methodologies, mechanism of formation, and their potential applications. Nanoscale Res Lett 16(1):97
4. European Union (EU). Commission recommendation of 18 October 2011, on the definition of nanomaterial (2011/696/EU), Official J. European Union. L275/38, 2011. https://eur-lex.europa.eu/legal-content/EN/TXT/?uri=CELEX:32011H0696. Accessed 13 Nov 2021
5. Jalab J, Abdelwahed W, Kitaz A, Al-Kayali R (2021) Green synthesis of silver nanoparticles using aqueous extract of *Acacia cyanophylla* and its antibacterial activity. Heliyon 7(9):e08033
6. Skiba M, Pivovarov A, Vorobyova V, Tetiana D, Iryna K (2019) Plasma- chemical formation of silver nanoparticles: the silver ions concentration effect on the particle size and their antimicrobial properties. J Chem Technol Metall 4(2):311–318
7. Vanlalveni C, Lallianrawna S, Biswas A, Selvaraj M, Changmai B, Rokhum SL (2021) Green synthesis of silver nanoparticles using plant extracts and their antimicrobial activities: a review of recent literature. RSC Adv 11:2804–2837
8. Mourdikoudis S, Pallares RM, Thanh NTK (2018) Characterization techniques for nanoparticles: comparison and complementarity upon studying nanoparticle properties. Nanoscale 10(27):12871–12934
9. Moradi R, Sebt SA, Karimi-Maleh H, Sadeghi R, Karimi F, Bahari A, Arabi H (2013) Synthesis and application of FePt/CNTs nanocomposite as a sensor and novel amide ligand as a mediator for simultaneous determination of glutathione, nicotinamide adenine dinucleotide, and tryptophan. Phys Chem Chem Phys 15(16):5888–5897
10. Chung IM, Park I, Seung-Hyun K, Thiruvengadam M, Rajakumar G (2016) Plant-mediated synthesis of silver nanoparticles: their characteristic properties and therapeutic applications. Nanoscale Res Lett 11(1):40
11. Ahmed S, Ahmad M, Swami BL, Ikram S (2016) A review on plant extracts mediated synthesis of silver nanoparticles for antimicrobial applications: a green expertise. J Adv Res (7)1:17–28
12. Khan MZH, Tareq FK, Hossen MA, Roki MNA (2018) Green synthesis and characterization of silver nanoparticles using *Coriandrum sativum* leaf extract. J Eng Sci Technol 13(1):158–166

13. Abdi V, Sourinejad I, Yousefzadi M, Ghasemi Z (2018) Mangrove-mediated synthesis of silver nanoparticles using native *Avicennia marina* plant extract from southern Iran. Chem Eng Commun 205(8):1069–1076
14. Jalani NS, Zati-Hanani S, Teoh YP, Abdullah R (2018) Short review: the effect of reaction conditions on plant-mediated synthesis of silver nanoparticles. Mater Sci Forum 917:145–151
15. Prasad TNVKV, Kambala VSR, Naidu R (2013) Phyconanotechnology: synthesis of silver nanoparticles using brown marine algae *Cystophora moniliformis* and their characterization, J Appl Phycol 25:177–182
16. Haleemkhan AA, Naseem, Vardhini BV (2015) Synthesis of nanoparticles from plant extracts. Int J Mod Chem Appl Sci 2(3):195–203
17. Mladenova B, Diankov S, Karsheva M, Stankov S (2018) Plant mediated synthesis of silver nanoparticles using extracts from *Tilia cordata*, *Matricaria chamomilla*, *Calendula officinalis*, and *Lavandula angustifolia* flowers. J Chem Technol Metall 53(4):623–630
18. Malik P, Shankar R, Malik V, Sharma N, Mukherjee TK (2014) Green chemistry based benign routes for nanoparticle synthesis. J Nanopart 2014:1–14
19. Abdel-Hafez SI, Nafady NA, Abdel-Rahim IR, Shaltout AM, Daròs AJ, Mohamed MA (2016) Assessment of protein silver nanoparticles toxicity against pathogenic *Alternaria solani*. 3 Biotech 6(2):199
20. He Y, Du Z, Ma S, Cheng S, Jiang S, Liu Y, Li D, Huang H, Zhang K, Zheng X, (2016) Biosynthesis, antibacterial activity and anticancer effects against prostate cancer (PC-3) cells of silver nanoparticles using *Dimocarpus Longan Lour*. peel extract. Nanoscale Res Lett 11(1):300
21. Madkour LH (2018) Ecofriendly green biosynthesized of metallic nanoparticles: bio-reduction mechanism, characterization and pharmaceutical applications in biotechnology industry. Glob Drug Therap 3(1):1–11
22. Mousavi SAA, Pourtalebi S (2015) Inhibitory effects of silver nanoparticles on growth and Aflatoxin B1 production by *Aspergillus parasiticus*, Iran J Med Sci 40(6):501–506
23. Banerjee P, Satapathy M, Mukhopahayay A, Das P (2014) Leaf extract mediated green synthesis of silver nanoparticles from widely available Indian plants: synthesis, characterization, antimicrobial property, and toxicity analysis. Bioresourc Bioprocess 1(1):1–10
24. Yadav R, Agarwala M (2011) Phytochemical analysis of some medicinal plants. J Phytol 3(12):10–14
25. Samejo MQ, Sumbul A, Shah S, Memon SB, Chundrigar S (2013) Phytochemical screening of *Tamarix dioica Roxb*. ex Roch. J Pharm Res 7(2):181–183
26. Yadav M, Chatterji S, Gupta SK, Watal W (2014) Preliminary phytochemical screening of six medicinal plants used as traditional medicine. Int J Pharm Pharm Sci 6(5)539–542
27. Baoduy LN, Trang DTD, Trang NPM (2015) Preliminary phytochemical analysis of leaf extracts *Ofthuja orientalis* (*L*.) ENDL. Int J Res Sci Manag 2(1):21–25
28. Chaudhuri SK, Chandela S, Malodia L (2016) Plant mediated green synthesis of silver nanoparticles using *Tecomella undulata* leaf extract and their characterization. Nano Biomed Eng 8(1):1–8
29. El-Kassas HY, Komi MME (2014) Biogenic silver nanoparticles using seaweed *Ulva rigida* and their fungicidal and cytotoxic effects. J of King Abdulaziz Univ: Mar Sci 25(1):3–20
30. Manivasagan P, Venkatesan J, Senthilkumar K, Sivakumar K, Kim SK (2013) Biosynthesis, antimicrobial and cytotoxic effect of silver nanoparticles using a novel *Nocardiopsis sp.* MBRC-1. Biomed Res Int 2013:287638
31. Skandalis N, Dimopoulou A, Georgopoulou A, Gallios N, Papadopoulos D, Tsipas D, Theologidis I, Michailidis N, Chatzinikolaidou M (2017) The effect of silver nanoparticles size, produced using plant extract from *Arbutus unedo*, on their antibacterial efficacy. Nanomaterials (Basel) 7(7):178
32. Chiguvare H, Oyedeji OO, Matewu R, Aremu O, Oyemitan IO, Oyedeji AO, Nkeh-Chungag BN, Songca SP, Mohan S, Oluwafemi OS (2016) Synthesis of silver nanoparticles using buchu plant extracts and their analgesic properties. Molecules 2(6):774

33. Pirtarighat S, Ghannadnia M, Baghshahi S (2019) Green synthesis of silver nanoparticles using the plant extract of *Salvia spinosa* grown in vitro and their antibacterial activity assessment. J Nanostruct Chem 9:1–9
34. Krishnaraj C, Harper SL, Choe HS, Kim KP, Yun SI (2015) Mechanistic aspects of biologically synthesized silver nanoparticles against food- and water-borne microbes. Bioprocess Biosyst Eng 38(10):1943–1958
35. Vivek M, Kumar PS, Steffi S, Sudha S (2011) Biogenic silver nanoparticles by *Gelidiella acerosa* extract and their antifungal effects. Avicenna J Med Biotechnol 3(3):143–148
36. Behera S, Nayak PL (2013) In vitro antibacterial activity of green synthesized silver nanoparticles using Jamun extract against multiple drug resistant bacteria. World J Nano Sci Technol 2(1):62–65
37. Mishra MM, Sahoo SS, Naik GK, Parida K (2015) Biomimetic synthesis, characterization and mechanism of formation of stable silver nanoparticles using *Averrhoa carambola L*. leaf extract. Mater Lett 160:566–571
38. Carmona ER, Benito N, Plaza T, Recio-Sánchez G (2017) Green synthesis of silver nanoparticles by using leaf extracts from the endemic *Buddleja globosa* hope, Green Chem Lett Rev 10(4):250–256
39. Zhang XF, Liu ZG, Shen W, Gurunathan S (2016) Silver nanoparticles: Synthesis, characterization, properties, applications, and therapeutic approaches. Int J mol Sci 17(9):1534
40. Okafor F, Janen A, Kukhtareva T, Edwards V, Curley M (2013) Green synthesis of silver nanoparticles, their characterization, application, and antibacterial activity. Int J Environ Res Public Health 10(10):5221–5238
41. Kassama SL, Kuponiyi AJ, Kukhtareva T (2015) Comparative effects of Aloe Vera (*Aloe Barbadensis*) water vs ethanol extracts on the physicochemical properties and stability of silver nanoparticles synthesize. American Int J Contemp Res 5(2):30–39
42. Sharma K, Guleria S, Razdan VK (2020) Green synthesis of silver nanoparticles using *Ocimum gratissimum* leaf extract: characterization, antimicrobial activity, and toxicity analysis. J Plant Biochem Biotechnol 29:213–224
43. Singh M, Kumar M, Kalaivani R, Manikandan S, Kumaraguru SK (2013) Metallic silver nanoparticle: a therapeutic agent in combination with antifungal drug against human fungal pathogen. Bioprocess Biosyst Eng 36(4):407–415
44. Anjum S, Abbasi BH, Shinwari ZK (2016) Plant-mediated green synthesis of silver nanoparticles for biomedical applications: challenges and opportunities. Pakistan J Bot 48(4):1731–1760
45. Hamelian M, Zangeneh MM, Amisama A, Varmira K, Veisi H (2018) Green synthesis of silver nanoparticles using *Thymus kotschyanus* extract and evaluation of their antioxidant, antibacterial and cytotoxic effects. Appl Organomet Chem 32(9):1–8
46. Velmurugan P, Iydroose M, Lee SM, Cho M, Park JH, Balachandar V, Oh BT (2014) Synthesis of silver and gold nanoparticles using cashew nut shell liquid and its antibacterial activity against fish pathogens. Indian J Microbiol 4(2):196–202
47. Christensen L, Vivekanandhan S, Misra M, Mohanty AK (2011) Biosynthesis of silver nanoparticles using *murraya koenigii* (curry leaf): an investigation on the effect of broth concentration in reduction mechanism and particle size. Adv Mater Lett 2(6):429–434
48. Gavade NL, Kadam AN, Suwarnkar MB, Ghodake VP, Garadkar KM (2015) Biogenic synthesis of multi-applicative silver nanoparticles by using *Ziziphus Jujuba* leaf extract. Spectrochim Acta A Mol Biomol Spectrosc 36 Pt B:953–960
49. Jogee PS, Ingle AP, Rai M (2017) Isolation and identification of toxigenic fungi from infected peanuts and efficacy of silver nanoparticles against them. Food Control 71:143–151
50. Haider MJ, Mehdi MA (2014) Study of morphology and zeta potential analyzer for the silver nanoparticles. Int J Sci Eng Res 5(7):381–387
51. Anandalakshmi K, Venugobal J, Ramasamy V (2015) Characterization of silver nanoparticles by green synthesis method using *Pedalium murex* extract and their antibacterial activity. Appl Nanosci 6:399–408

Figures

Figure 1

Picture of healthy plants leaves and nuts used in the biosynthesis of AgNPs

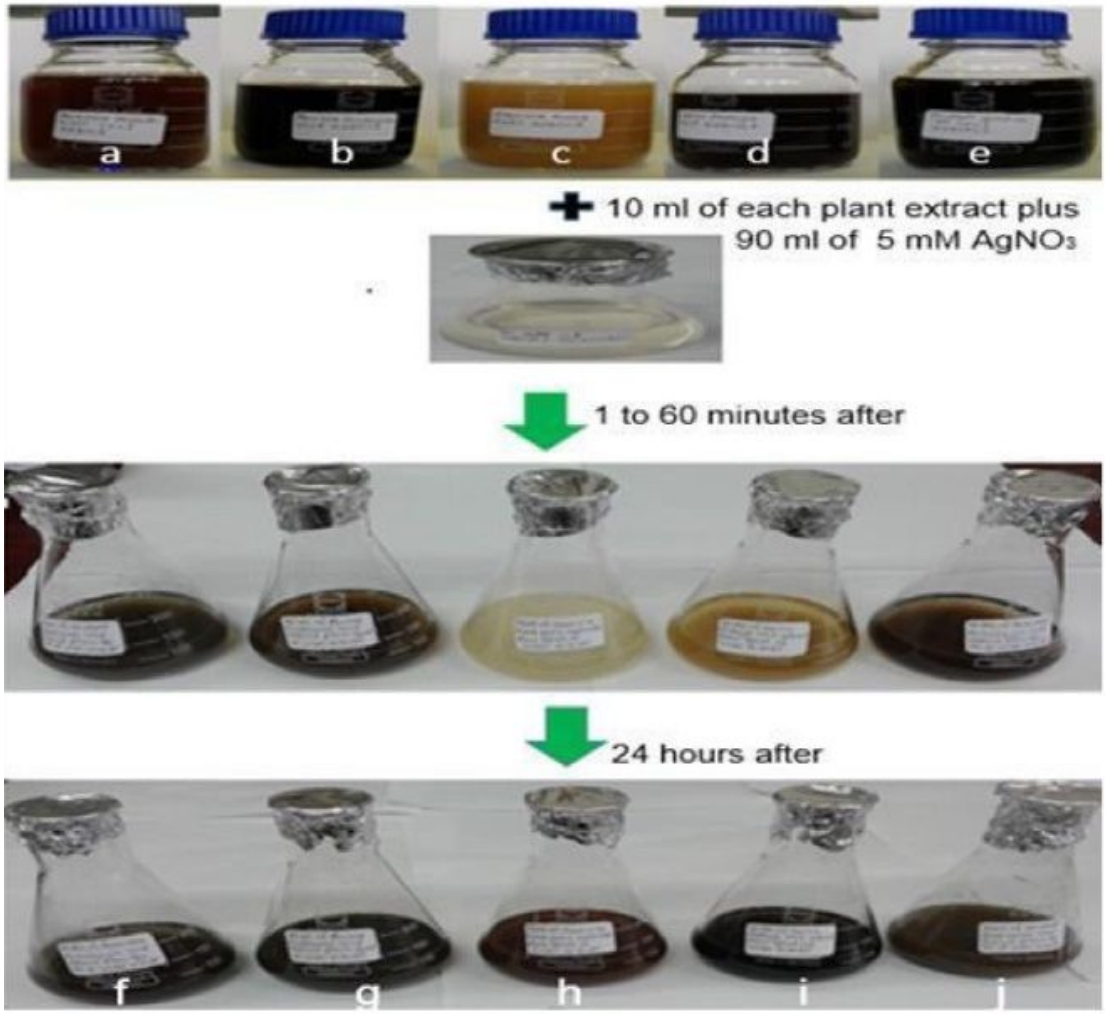

Figure 2

Observed color change in the reaction mixtures during biosynthesis of AgNPs using aqueous extracts of (a) Achillea millefolium, (b) Perilla frutescens, (c) Garcinia kola, (d) Carica papaya, and (e) Ocimum gratissimum

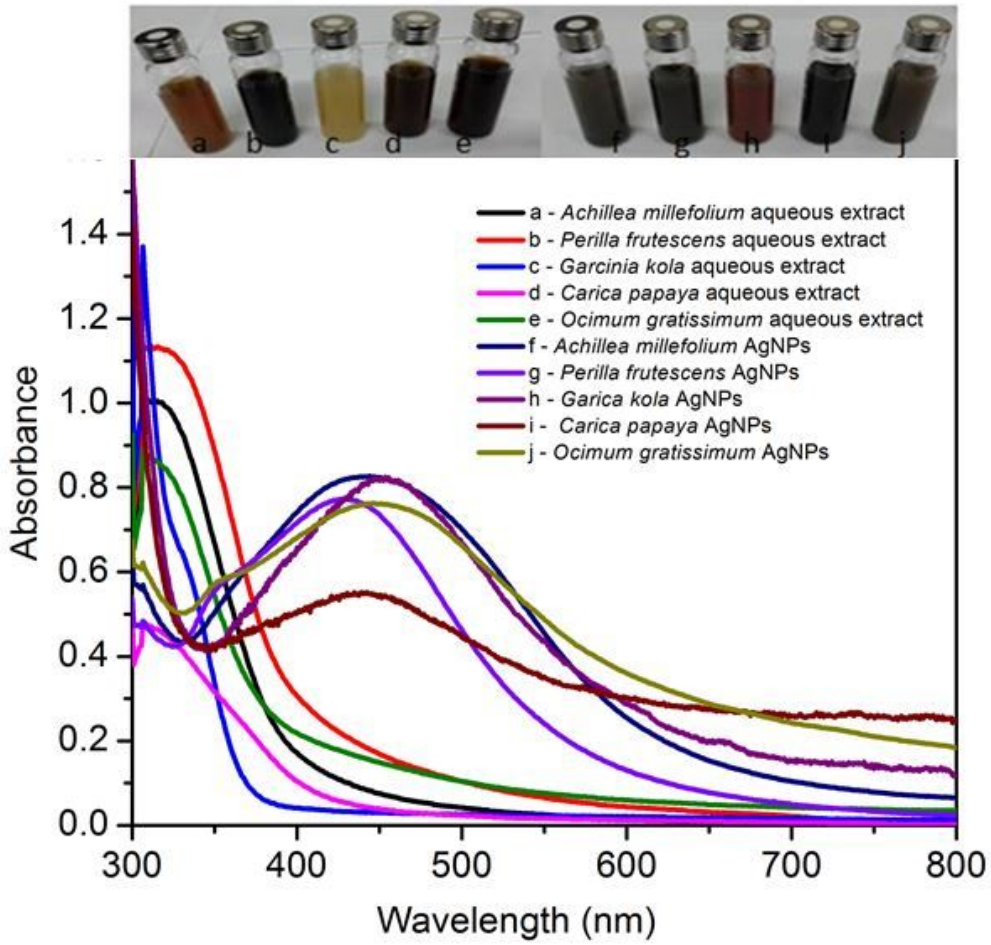

Figure 3

UV-Vis spectrum of (a) Achillea millefolium aqueous extract, (b) Perilla frutescens aqueous extract, (c) Garcinia kola aqueous extract, (d) Carica papaya aqueous extract, (e) Ocimum gratssimum aqueous extract, (f) Achillea millefolium AgNPs (g) Perilla frutescens AgNPs, (h) Garcinia kola AgNPs, (i) Carica papaya AgNPs, and (j) Ocimum gratssimum AgNPs

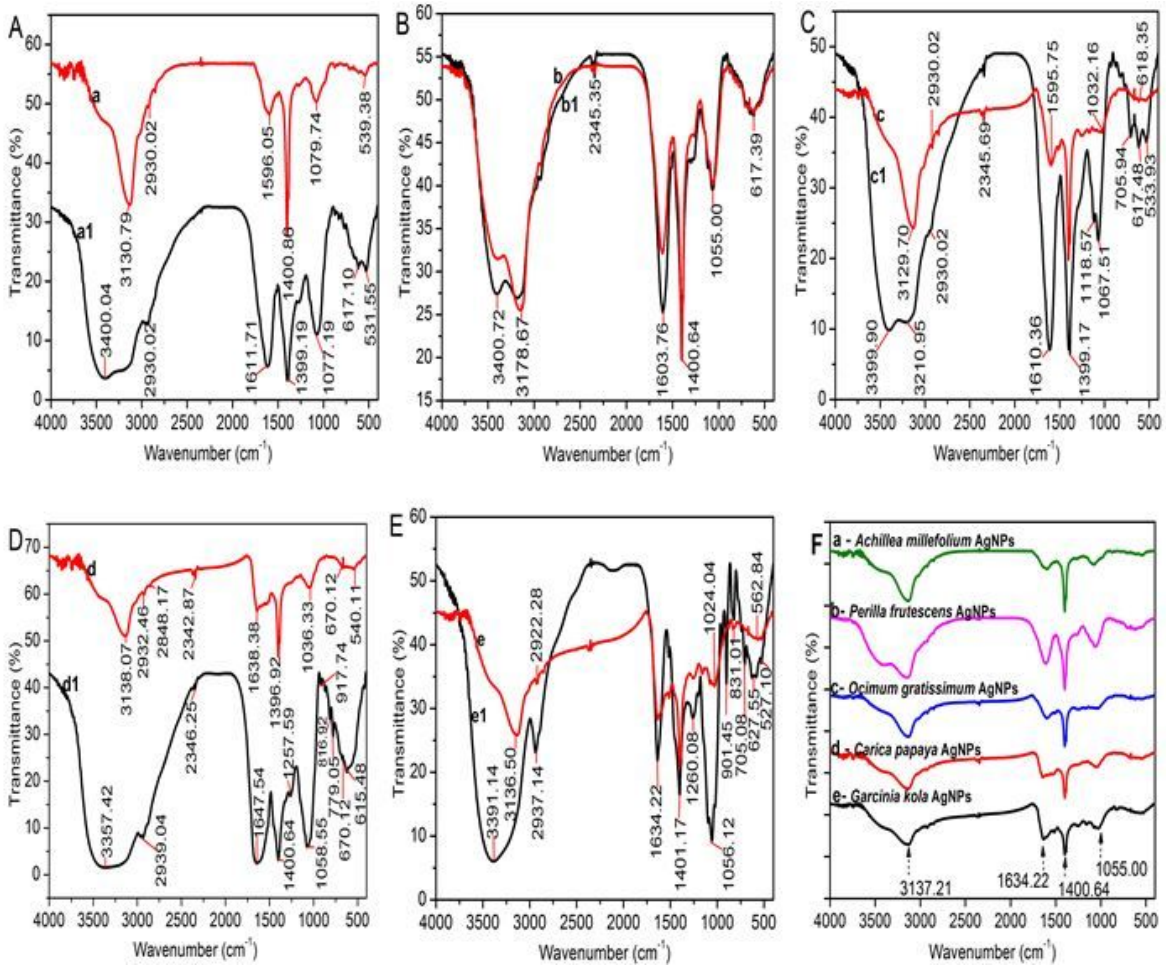

Figure 4

FTIR spectrum of A) (a) Achillea millefolium AgNPs, (a1) Achillea millefolium extract, B) (b) Perilla frutescens AgNPs, (b1) Perilla frutescens extract, C) (c) Ocimum gratissimum AgNPs, (c1) Ocimum gratissimum extract, D) (d) AgNPs by Carica papaya AgNPs, (d1) Carica papaya extract E) (e) Garcinia kola AgNPs, (e1) Garcinia kola extract, and (F) all the biosynthesized AgNPs (a, b, c, d, and e)

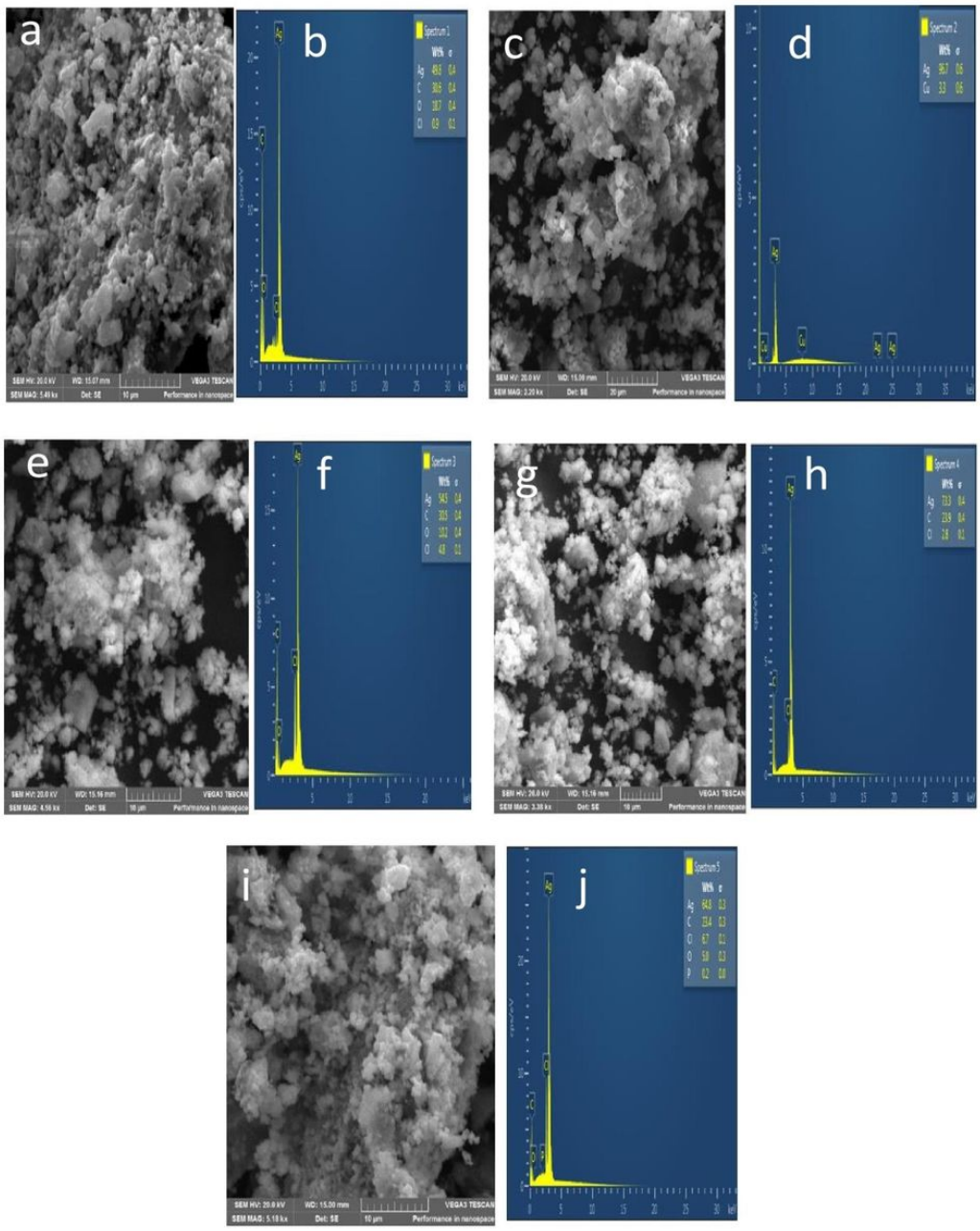

Figure 5

SEM/EDX results of biosynthesized AgNPs (a) SEM of Carica papaya AgNPs, (b) EDX of Carica papaya AgNPs, (c) SEM of Garcinia kola AgNPs, (d) EDX of Garcinia kola AgNPs, (e) SEM of Ocimum gratissimum AgNPs, (f) EDX of Ocimum gratissimum AgNPs, g) SEM of Perilla frutescens AgNPs, (h) EDX of Perilla frutescens AgNPs, (i) SEM of Achillea millefolium AgNPs, and (j) EDX of Achillea millefolium AgNPs

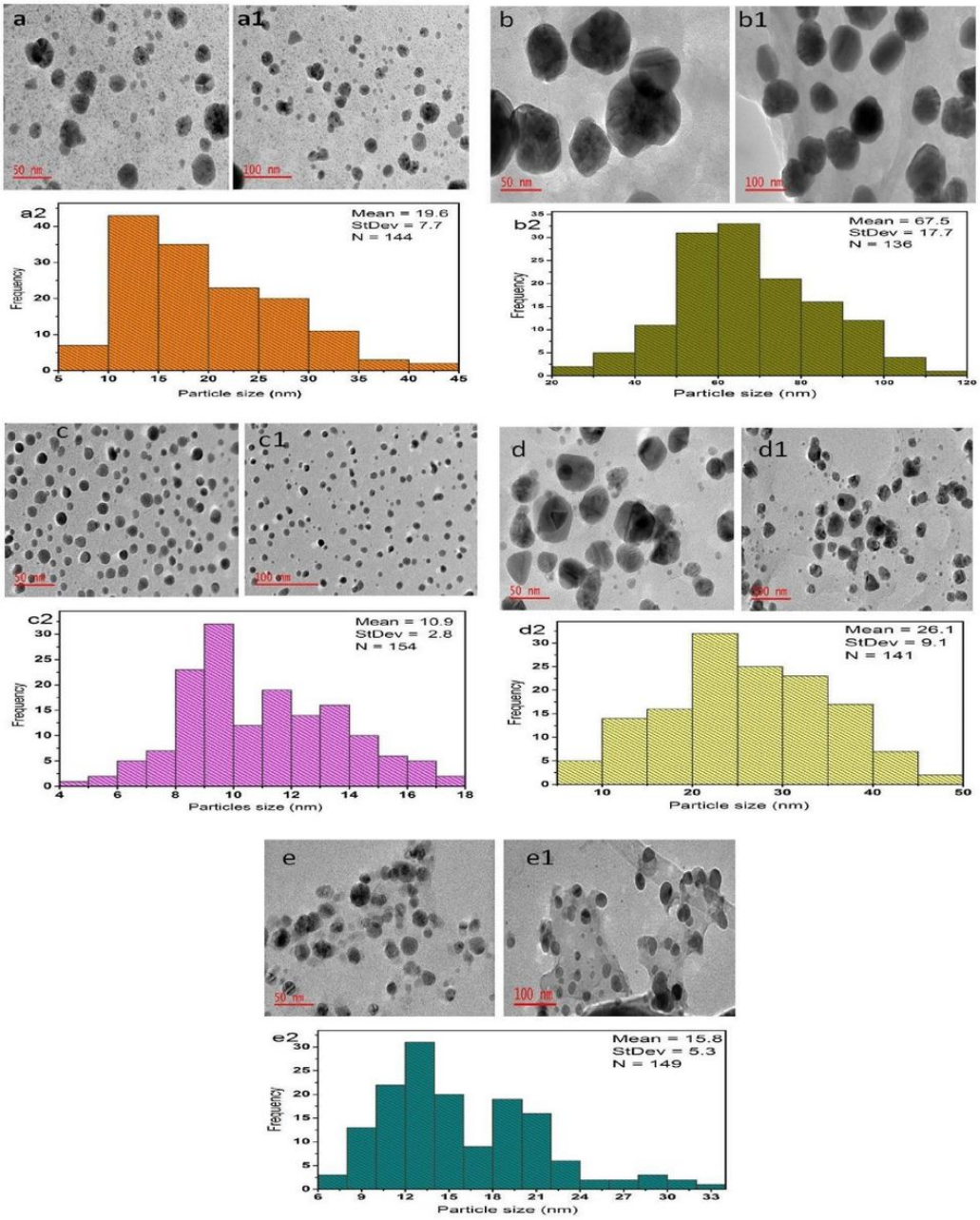

Figure 6

HRTEM micrographs of biosynthesized AgNPs taken at 50 and 100 nm for (a and a1) Garcinia Kola AgNPs, (b and b1) Carica papaya AgNPs, (c and c1) Achillea millefolium AgNPs, (d and d1) Perilla frutescens AgNPs, (e and e1) Ocimum gratissimum AgNPs. Particle size distribution histogram for (a2) Garcinia kola AgNPs, (b2) Carica papaya AgNPs, (c2) Achillea millefolium AgNPs (d2) Perilla frutescens AgNPs, and (e2) Ocimum gratissimum AgNPs

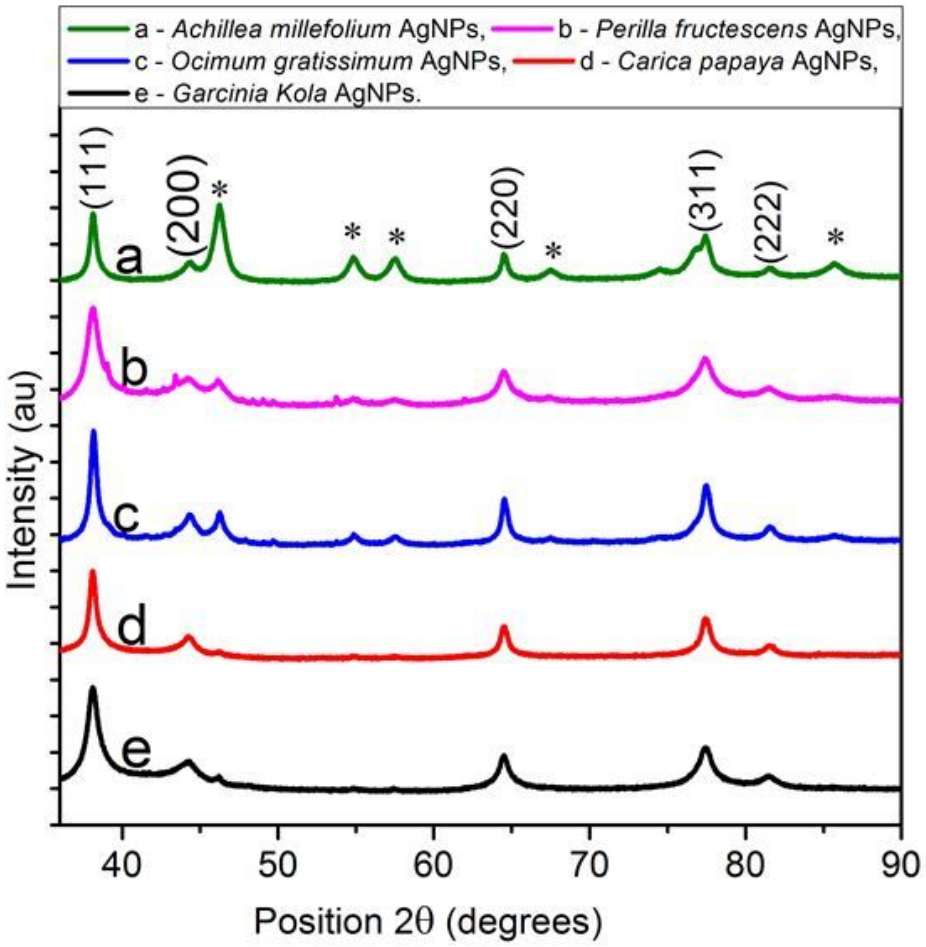

Figure 7

XRD pattern of AgNPs biosynthesized using (a) Achillea millefolium, (b) Perilla frutescens, (c) Ocimum gratissimum, (d) Carica papaya, and (e) Garcinia kola

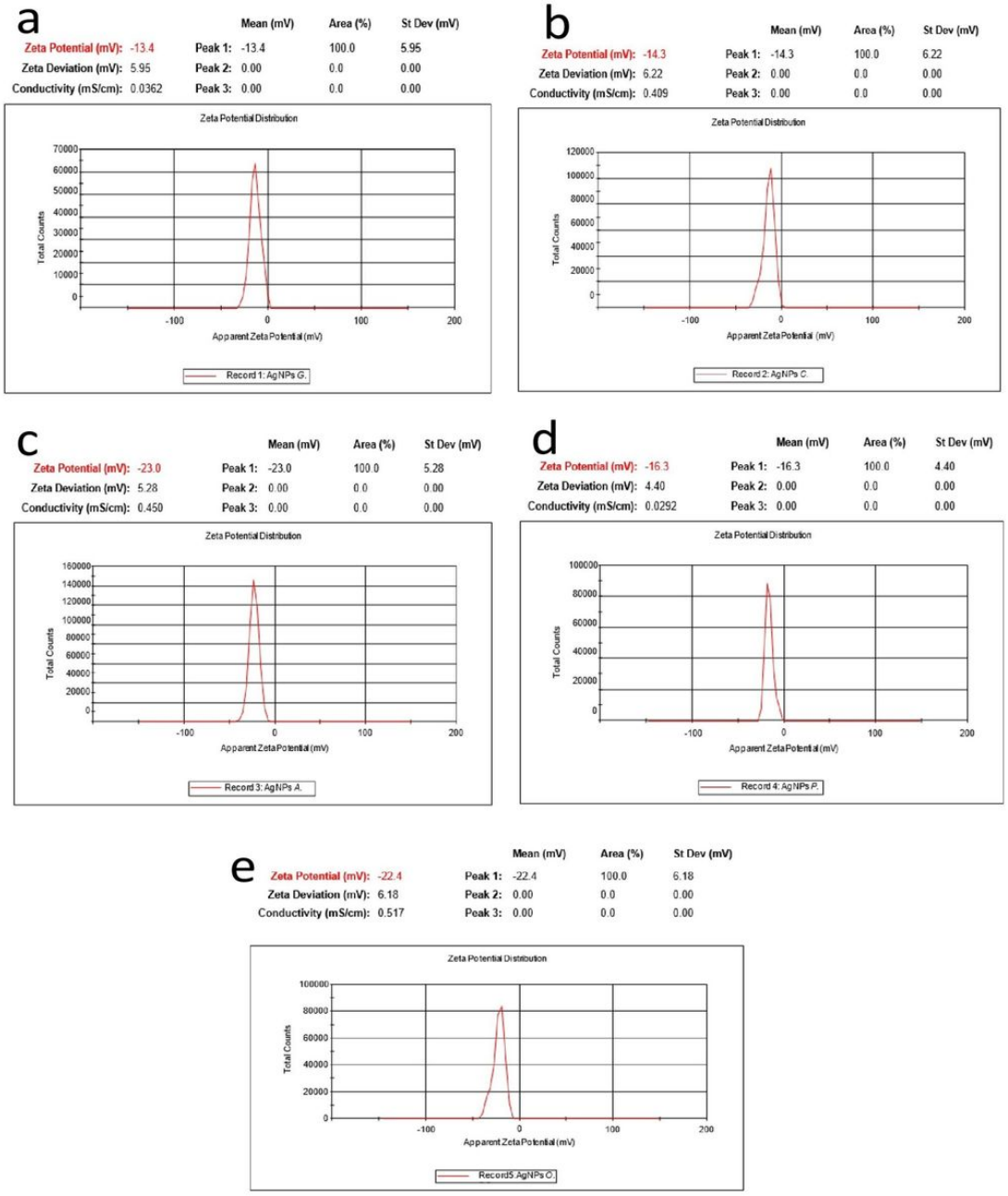

Figure 8

Zeta potential of (a) Garcinia kola, (b) Carica papaya, (c) Achillea millefolium, (d) Perilla frutescens, and (e) Ocimum gratissimum AgNPs